Progress In Electromagnetics Research B, Vol. 70, 87–100, 2016

Transferometry: A New Tool for Complex Wired Networks Diagnosis

Fabrice Auzanneau*

Abstract—Electrical cables of all types are subject to aggressive operational environments that can be source of defects or accelerated aging. Reflectometry-based methods are among the best ones for the detection and location of hard defects, but cannot easily provide efficient unambiguous diagnosis for complex topology networks, such as bus or star-shaped wired networks. This paper introduces the use of a new method, called transferometry, as an additional tool for the diagnosis of complex topology networks and shows that it presents many advantages compared to reflectometry, both in terms of implementation and data processing. Based on the fusion of the analysis results of several transmitted signals, it can provide a better diagnosis with fewer sensors than distributed reflectometry, with a simpler electronic architecture.

1. INTRODUCTION

Electric cables are widely used for energy and signal transmission in various application domains, and their reliability is of utmost importance as defects can have dramatic consequences in terms of system readiness, potential damage to equipments or the environment, and even casualties [1]. As an example, smart grids, modern energy distribution networks using heterogeneous sources and information systems for measurement, control and communication, become the most efficient energy infrastructures and heavily rely on monitoring systems to improve their performances. Deployed at various scales, from small districts up to wide countries, they require specific watch systems to ensure 24-hour reliable service [2]. Most monitoring systems use voltage or current measurement results to detect failures, but the cabling infrastructure also requires condition monitoring.

Many other domains exist that require wire diagnosis systems as well, such as transports, industry and buildings, railway infrastructures, health equipments, nuclear power plants, etc. To decrease maintenance and immobilization costs, it is important to quickly detect and precisely locate failures in wired networks, even in the case of networks of complex topologies.

Among various diagnosis methods, the most efficient one is reflectometry [3]. High frequency electrical method similar to RADAR, reflectometry injects a probing signal into only one end of the cable under test: if during propagation the signal meets an impedance discontinuity, part of its energy is sent back to the injection port, while the rest keeps propagating in the cable. In standard reflectometry methods, the analysis of the reflected signals provides information on the presence and location of the back-scatterers, which can be junctions, connectors, loads or defects. Reflectometry includes two main families: Time Domain Reflectometry (TDR) and Frequency Domain Reflectometry (FDR). TDR is the easiest to understand: a sensor periodically injects the probe signal at one end of the network under test and measures a signal which is made of multiple copies delayed in time. For each copy, the delay is the round trip time necessary to reach the discontinuity from the injection point. This composite signal is called "reflectogram". If one knows the propagation velocity, one can locate the discontinuity or defect which created each copied signal, and the shape and amplitude of this signal provide information on the nature of the defect. Several versions have been proposed, from M-STDR

Received 6 July 2016, Accepted 9 October 2016, Scheduled 21 October 2016
* Corresponding author: Fabrice Auzanneau (fabrice.auzanneau@cea.fr).
The author is with the CEA, LIST, CEA Saclay Nano-INNOV, PC 172, F-91191 Gif sur Yvette, France.

(Modified Sequence Time Domain Reflectometry) [4], MCTDR (Multi Carrier TDR) [5] to the recent OMTDR (Orthogonal Multi Tone TDR) method [6] inspired by OFDM (Orthogonal Frequency-Division Multiplexing) communication technique. FDR [7] injects a set of sine waves in the cable and analyses the standing wave made of the superposition of the injected and reflected signals. This analysis is quite easy for a simple point to point cable but it becomes complicated for complex networks.

All these methods have their own advantages and drawbacks, and they provide high performance defect detection (see [1] for comparison) and location accuracy of less than 1% of the length of the cable under test. But high frequency signal propagation in cables suffer from attenuation and dispersion which make it difficult to diagnose km-long cables. Even using specific techniques, such as self-adaptive correlation [8] or model-based compensation [9], it may be difficult to precisely detect and locate far away defects that have a very low signature. Moreover, complex branched networks, as can be found in smart grids for energy distribution, increase this difficulty as propagating signals are attenuated when they cross a junction. Specific distributed diagnosis methods have been proposed [10, 11] to address this problem by connecting reflectometers at several ends of the network, adding the need for communication among this sensor network. Of course, all the signals must not interfere with each other, which is made possible for example by the recent CTDR (Chaos TDR) method [12].

But all these methods share the same basis: defects are detected and localized through the analysis of the signals reflected by the cable at each injection port. Distributed diagnosis began to change the concept by adding several sensors, but these methods still rely on the analysis of the signals they inject and do not take benefit of the other signals. To bypass this limitation and take advantage of the additional information propagated by the other sensors signals, we present in this paper a new diagnosis method called Transferometry. Each sensor receives and processes the signals generated by all the sensors connected to the network under test, including himself, and sensor fusion enables to further enrich the analysis results. The information obtained after signal processing is called a *transferogram*.

Recently, some innovative works have applied the time reversal principles, first developed in [13], to the detection and location of defects in wire networks. Time reversal takes advantage of the independence of the propagation equations to the sign of time to focus scattered waves back to their original source. This is done in 2 phases: first measure the transferred waves at several places on the boundary of the propagation space, and then reverse them in time and propagate these new waves again from the measurement points. A scattering matrix relates injected and measured waves of phase 1, and is used to define a time reversal operator whose eigenvectors generate the new waves of phase 2. This is called the DORT (Decomposition de l'Operateur de Retournement Temporel) method [14], and has been applied to the location of multiple defects in wire networks [15]. One drawback of this method is that the focusing phase can only be done using numerical simulation, which may result in reduced accuracy. Transferometry only measures the transferred waves and does not require any additional propagation phase. To the best of our knowledge, the transferometry method has never been presented before for wire diagnosis application.

This paper is organized as follows. Section 2 presents the principles of transferometry, and Section 3 provides a theoretical model for signal propagation and transferogram simulation. Then Section 4 will show some numerical results on various complex topology networks, followed by a discussion in Section 5 showing the new method's advantages. Section 6 concludes the paper.

2. TRANSFEROMETRY'S PRINCIPLE

The principle used in transferometry is that the sensors watching the network can emit, receive and process signals. Similar to reflectometers, they generate their own signal, inject it into the network and process the signal coming back to them. But if they could moreover isolate the signals sent by the other sensors, and organize them to extract additional information, this would give a more global image of the network.

As a metaphor, if standard reflectometry is scalar while Distributed Reflectometry (DR) is vectorial, then transferometry is matricial. If N sensors are distributed over a wired network, then DR only uses N different data, and sends them to the main reflectometer which aggregates them and provides the diagnosis' result. Figure 1 shows that if N sensors are watching a wired network, transferometry utilizes up to $N(N+1)/2$ data. Using a greater amount of data, the diagnosis provided by transferometry is

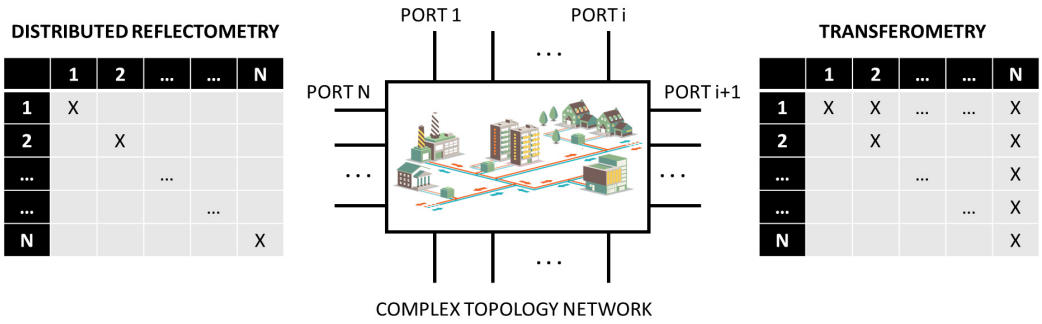

Figure 1. Applied to a complex topology network, transferometry provides a diagnosis based on much more information than simple or distributed reflectometry.

much richer than that of reflectometry.

If no communication means exists in the sensor's network, DR is not very efficient, as all sensors diagnose the network from their own viewpoints, but no fusion is done. For transferometry, the configuration is slightly different: $N-1$ 'slave' sensors inject their signals, which are received by the 'master' who can aggregate them to make a global diagnosis. Then, N data are processed, but they are different from those of DR. We will see in Section 5 that, in some cases, this degraded configuration can even provide a better diagnosis than reflectometry.

A prerequisite for transferometry is that the master sensor can easily separate and recognize the signals arriving from the other sensors. Standard technologies of channel access for shared medium networks [16] can be used for that: Time Division Multiple Access (TDMA), Frequency Division Multiple Access (FDMA) or Code Division Multiple Access (CDMA). FDMA principles are used in MCTDR or OMTDR methods, while CDMA principles are used by STDR and CTDR. The latter method enables to create a quasi infinite number of uncorrelated signals: as such, it will be the preferred method in the following sections.

3. THEORETICAL MODEL

3.1. *ABCD* Matrix of a Single Line

To compute the transmitted wave in a wire, the scattering parameters formalism seems the most suitable. The scattering matrix relates outgoing and incoming waves in a portion of the wire of length l, considered as a quadripole:

$$\begin{bmatrix} S_{11} & S_{12} \\ S_{21} & S_{22} \end{bmatrix} = \begin{bmatrix} 0 & e^{-\gamma l} \\ e^{-\gamma l} & 0 \end{bmatrix} \tag{1}$$

where γ is the propagation constant, given by [17]:

$$\gamma(\omega) = \sqrt{(R + jL\omega) \cdot (G + jC\omega)} \tag{2}$$

with $j^2 = -1$ and $\omega = 2\pi f$ the pulsation. The lumped elements R and L account for loss and energy storage in the conductors, C and G for insulation and loss in the insulator.

But this model is not suited for branched cables, and transferometry provides much more interesting results in branched networks. We then use the chain matrix formalism, defined by (see Figure 2 for notations):

$$\begin{bmatrix} V \\ I \end{bmatrix} = \begin{bmatrix} A & B \\ C & D \end{bmatrix} \cdot \begin{bmatrix} V' \\ I' \end{bmatrix}. \tag{3}$$

The $ABCD$ matrix of a line of length l is given by (4):

$$\begin{bmatrix} A & B \\ C & D \end{bmatrix} = \begin{bmatrix} \cosh \gamma l & Z_c \sinh \gamma l \\ \dfrac{\sinh \gamma l}{Z_c} & \cosh \gamma l \end{bmatrix}. \tag{4}$$

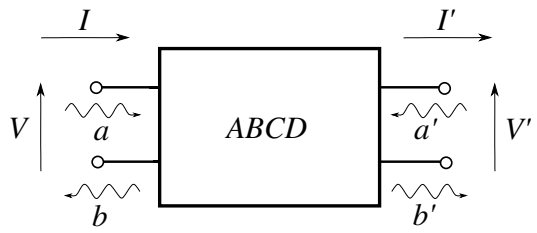

Figure 2. Notations for the $ABCD$ formalism.

where Z_c is the characteristic impedance of the line,

$$Z_c = \sqrt{\frac{R + jL\omega}{G + jC\omega}} \tag{5}$$

and matrices of contiguous line sections are cascaded as follows:

$$\begin{bmatrix} A & B \\ C & D \end{bmatrix} = \begin{bmatrix} A & B \\ C & D \end{bmatrix}_1 \cdot \begin{bmatrix} A & B \\ C & D \end{bmatrix}_2 \cdot \begin{bmatrix} A & B \\ C & D \end{bmatrix}_3 \tag{6}$$

The waves a, b, a' and b' are related to currents and voltages by:

$$\begin{cases} V = a + b & Z_c I = a - b \\ V' = a' + b' & -Z_c I' = a' - b' \end{cases} \tag{7}$$

Equations (7) have been simplified for easier use later in the paper. Using Equations (2) to (7) and appropriate boundary conditions, we can compute all incoming and outgoing waves. Then, the transmission coefficient between sensor i and sensor j is equal to:

$$T_{ij} = \frac{b_j}{a'_i}, \quad a'_k = 0 \quad \forall k \neq i \tag{8}$$

Note that $T_{ij} = T_{ji}$.

3.2. *ABCD* Matrix of a Branched Path

We now consider the case of N connected lines as shown in Figure 3. Applying Equation (3) to each line i gives:

$$Y_i = \frac{I_i}{V_i} = \frac{D_i - C_i Z_i}{B_i - A_i Z_i} \quad i = 2 \ldots N-1 \tag{9}$$

where Z_i is the load impedance of line i. Equation (9), together with Kirchhoff's relations at point B [18]

$$\begin{cases} V'_1 = V_i, & i = 2 \ldots N \\ I'_1 = \sum_{i=2}^{N} I_i \end{cases} \tag{10}$$

and the first line of Equation (3) applied to line N:

$$V_N = A_N V'_N + B_N I'_N \tag{11}$$

lead to the global $ABCD$ matrix of the quadripole AD:

$$\begin{bmatrix} V_1 \\ I_1 \end{bmatrix} = \begin{bmatrix} A_1 & B_1 \\ C_1 & D_1 \end{bmatrix} \begin{bmatrix} A_N & B_N \\ A_N \sum_{i=2}^{N} Y_i + C_N & B_N \sum_{i=2}^{N} Y_i + D_N \end{bmatrix} \begin{bmatrix} V'_N \\ I'_N \end{bmatrix} \tag{12}$$

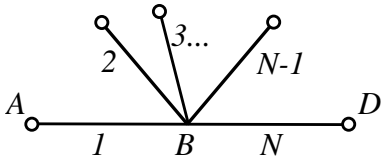

Figure 3. A branched path from D to A.

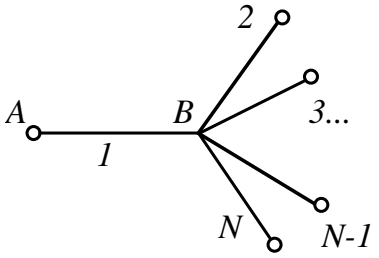

Figure 4. A branched sub-network, lines 2 to N are loaded.

3.3. *ABCD* Matrix of a Parallel Branched Sub-network

We consider a "branched dead-end" as shown in Figure 4, a smaller sub-network not on the direct path between the sensors. Similar maths provide the following formula for the equivalent admittance:

$$Y_s = \frac{C_1 + D_1 \sum_{i=2}^{N} Y_i}{A_1 + B_1 \sum_{i=2}^{N} Y_i} \tag{13}$$

where Y_i are computed using Equation (9).

3.4. *ABCD* Matrix of a Complex Topology Network

To compute the transmission coefficient between sensor i and sensor j, one must first draw the network around the direct path, then identify all network sections that can be simplified using Equation (13), and finally cascade all the "branched path" sections $ABCD$ matrices from i to j. This provides the equivalent $ABCD$ matrix of the path between the sensors, leading to an equation such as:

$$\begin{bmatrix} V_i \\ I_i \end{bmatrix} = \begin{bmatrix} A & B \\ C & D \end{bmatrix} \begin{bmatrix} V'_j \\ I'_j \end{bmatrix} \tag{14}$$

The transmission coefficient, as defined above, is then calculated using Equation (8):

$$T = \frac{Z_A + Z_c}{Z_c} \frac{AD - BC}{A + \frac{B}{Z_c} + CZ_A + D\frac{Z_A}{Z_c}} \tag{15}$$

where Z_A is the load impedance of the receiving sensor j. If the sensors has a high impedance, this simplifies to:

$$T = \frac{AD - BC}{CZ_c + D} \tag{16}$$

3.5. An Example

Figure 5 shows an example of a complex topology network with reflectometry sensors at ports A and B. The left part presents the physical topology, and the right part shows the network organized around the direct path between sensors. Sections 3.1 and 3.2 are parallel branched sub-networks, and their respective equivalent admittances can be obtained using Equation (13) as follows.

Section 3.2 is divided into 3 subsections (as shown in Figure 6), where:

$$\begin{aligned} Y_{3.2.1} &= \frac{C_4 + D_4(Y_1 + Y_2 + Y_3)}{A_4 + B_4(Y_1 + Y_2 + Y_3)} \\ Y_i &= \frac{D_i - C_i Z_i}{B_i - A_i Z_i}, \quad i = 1 \ldots 3 \\ Y_{3.2.2} &= \frac{D_5 - C_5 Z_5}{B_5 - A_5 Z_5} \\ Y_{3.2} &= \frac{C_6 + D_6(Y_{3.2.1} + Y_{3.2.2})}{A_6 + B_6(Y_{3.2.1} + Y_{3.2.2})} \end{aligned} \tag{17}$$

and a similar process can be applied to Section 3.1.

Then Equation (12) is used successively in Sections 1 and 2 (with $N = 3$), and, knowing $Y_{3.1}$ and $Y_{3.2}$, again Equation (12) provides the final equivalent $ABCD$ matrix of the network. The transmission coefficient is obtained using Equation (15).

Of course, the transmission coefficient is computed for each frequency in the considered band, and an inverse Fourier transform provides the transferogram in the time domain. The transferogram can then be plotted vs. distance, knowing the velocity of propagation of waves in the cables.

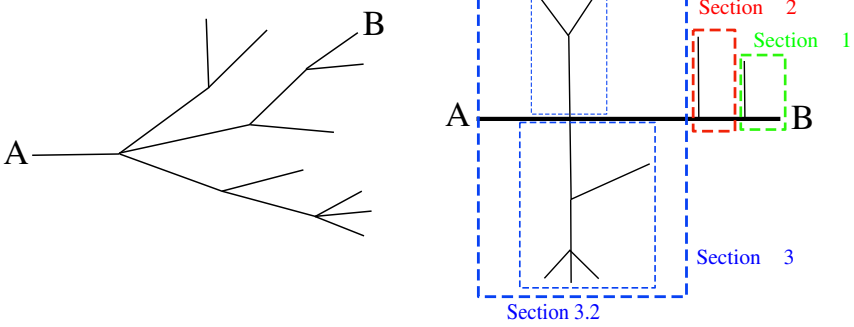

Figure 5. Decomposition of the network's topology.

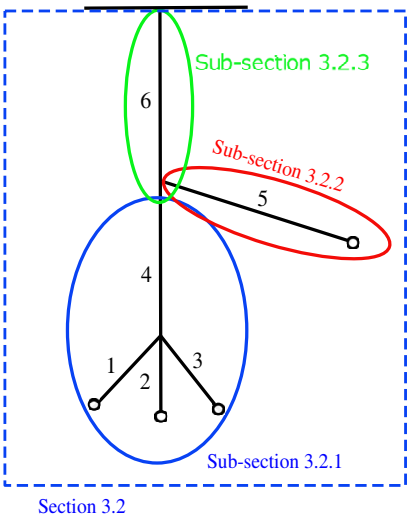

Figure 6. Decomposition of Section 3.2.

4. NUMERICAL RESULTS

4.1. Bus-Type Network

We consider a first network topology taken from [19], shown in Figure 7. Table 1 provides the length of each wire. We suppose that the network is monitored by 3 sensors, placed at points A, B and C. All lines are terminated by a high impedance load.

Table 1. Lengths of wires on the bus network of Figure 7 (in meters).

L_1	L_2	L_3	L_4	L_5	L_6	L_7
4.6	8.1	15	14	30	31.5	16

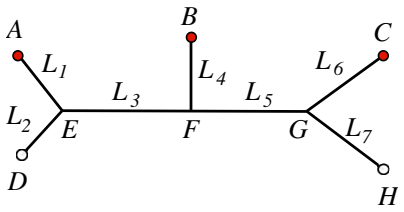

Figure 7. Bus-type network topology.

For a junction as shown in Figure 3, if all lines have the same characteristic impedance, the local reflexion and transmission coefficients at point B are given by:

$$\begin{aligned} R_N &= \frac{2-N}{N} \\ T_N &= \frac{2}{N} \end{aligned} \tag{18}$$

If we suppose that an open circuit defect is created on line L_7, we get the following results:

- A reflectometer at point A won't detect the problem, as the defect's signal is attenuated by a factor $T_3^6 = (2/3)^6 \simeq 0.09$ and lost among a great number of peaks of larger amplitude,
- A reflectometer at point B may detect the defect, but will not be able to decide whether it is placed on line L_6 or line L_7 (ambiguous detection),
- A reflectometer at point C will detect and unambiguously locate the defect.

Such a branched network requires at least 3 reflectometers to provide a precise diagnosis [20]. More generally, a reflectometer cannot reliably detect defects after 3 junctions: a complex bus network requires at least that half the line ends are equipped with a reflectometer.

We now suppose that the 3 sensors are doing transferometry: sensor A is the master and sensors B and C are slaves (emitters). Figures 8 and 9 show the transferograms from respectively sensors B and C to sensor A: the main peaks are explained on the Figures.

An important remark is the following: the first peak on a transferogram corresponds to the direct path. Its amplitude can be predicted using Equation (18): the signal going from point B to point A must cross 2 junctions made of $N = 3$ lines, the direct path peak's amplitude is $T_3^2 = (2/3)^2 = 0.44\,\text{V}$. A transferogram direct path peak has always greater amplitude than the corresponding peak on a reflectogram, because the reflectometry's signal must cross twice as much junctions, due to round trip path.

The next peaks correspond to the reflections at the other lines ends: they are separated from the first peak by a distance equal to twice the length of the considered lines. As an example, the peak of the reflection at point B in Figure 9 is $2 \times L_4 = 28$ meters after the direct path's peak.

Figure 10 shows the transferogram from sensor C to sensor A after the defect is created. The first difference is situated at distance 105 m, i.e., 24 m after the direct path peak: this means that the defect is 12 meters away from a the direct path. Table 1 shows that line L_2 is too short and only lines L_4 and L_7 are candidate. But the peak of the reflection in B is still present, meaning that the defect is on line L_7. This is confirmed by the fact that the peak at 113 meters (reflection in H) drastically changed.

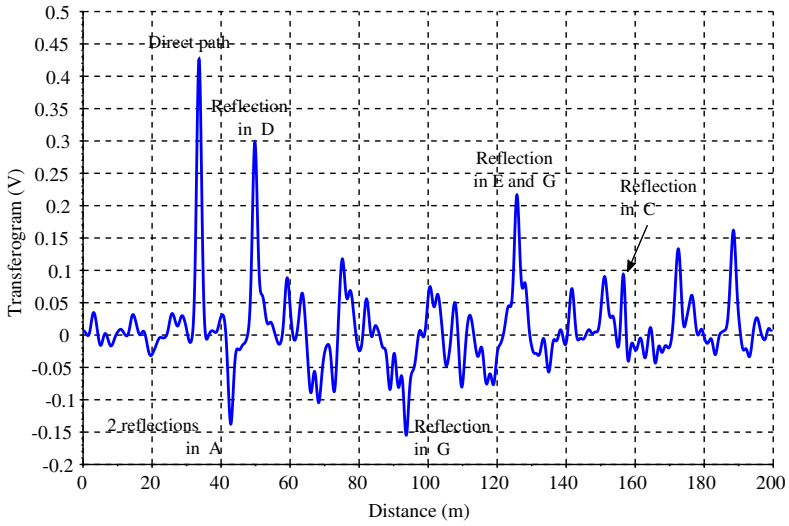

Figure 8. Transferogram from sensor B to sensor A before defect.

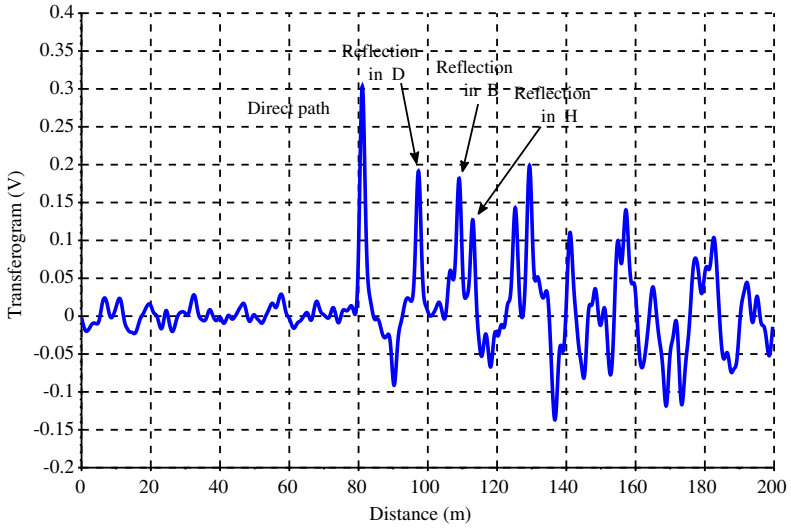

Figure 9. Transferogram from sensor C to sensor A before defect.

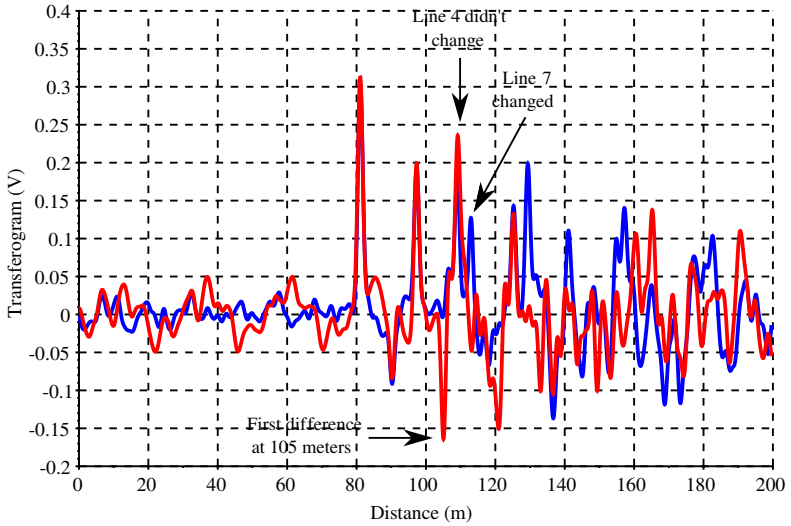

Figure 10. Transferogram from sensor C to sensor A after defect (red curve).

The difference between the transferograms of Figures 9 and 10 is plotted in Figure 11. A similar analysis can be done: the first difference greater than a threshold of amplitude ± 0.1 shows that the defect is 12 meters away from a the direct path, the second peak shows that line L_7 drastically changed.

This first test case shows that, in most cases, placing only one master and one slave transferometers at each end of a bus-type network is enough for unambiguous detection and location of hard defects. If several parallel lines have the same length, some additional slaves may be required.

4.2. Star-Shaped Network

We now consider a star-shaped network, as shown in Figure 12, similar to those used in buildings or infrastructures for energy distribution [21]. Equation (18) shows that the reflection coefficient at the junction is

$$R_8 = \frac{-3}{4} = -0.75 \tag{19}$$

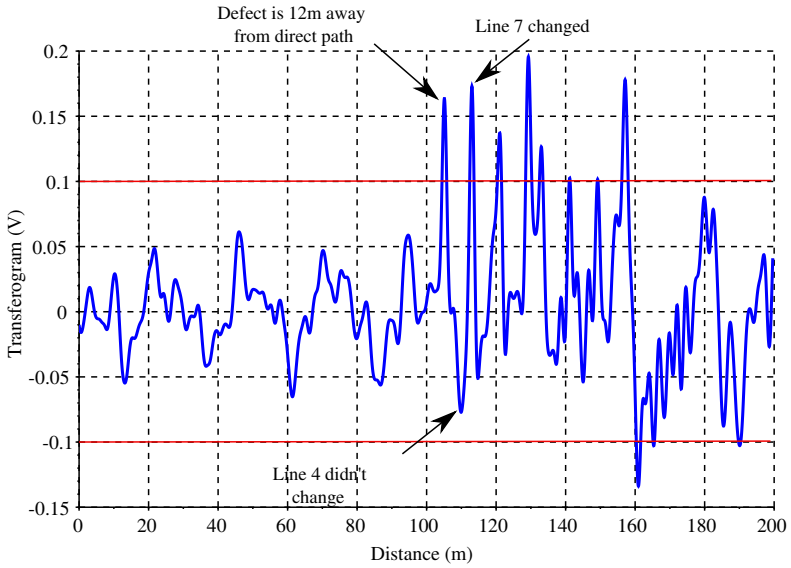

Figure 11. Difference between the transferogram from sensor C to sensor A before and after defect.

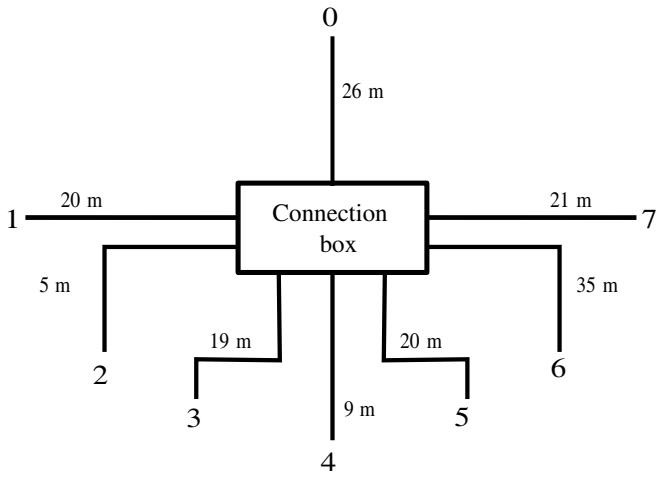

Figure 12. Star-shaped network topology.

then a single reflectometer will hardly be able to monitor any line beyond the connection box, as the attenuation due to double transmission would be $T_8^2 = 0.25^2 \simeq 0.06$. And even if it was accurate enough, lines 1, 3, 5 and 7 have very similar lengths which may cause location ambiguities (Figure 13): at least 4 reflectometers would be necessary to efficienlty monitor this network. The reflectogram in Figure 13 shows a great number of peaks due to multiple paths between branches of similar lengths. Clearly, reflectometry is not suited for the diagnosis of star-shaped networks.

Placing the sensors at the ends of lines of equal lengths is more efficient: we thus put 2 sensors at the end of lines 1 and 5. The transferogram from sensor 1 to sensor 5 is shown in Figure 14. It is much less complex than the reflectogram of Figure 13, as all the peaks are clearly identifiable. The direct path's length is 40 meters, leading to high amplitude peaks at 40, 80 and 120 meters.

We then simulate a short-circuit defect at the end of line 3. The new transferogram is compared to the previous one in Figure 15: the first visible difference is at distance 78 meters, meaning that the defect is $(78 - 40)/2 = 19$ meters away from the direct path. The amplitude of the direct path's peak didn't change, this means that the defect is not on lines 1 and 5: lines 3, 6 and 7 are the remaining candidates. But the peaks of lines 6 and 7 didn't change, meaning that the defect is on line 3.

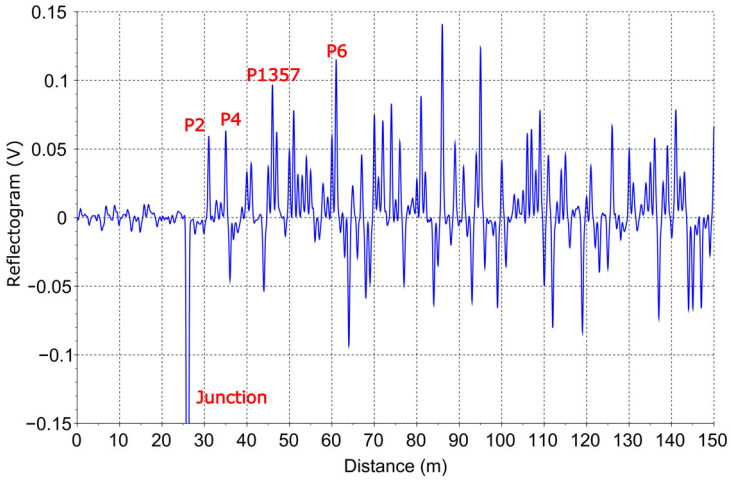

Figure 13. Reflectogram measured at point 0 on the star-shaped network.

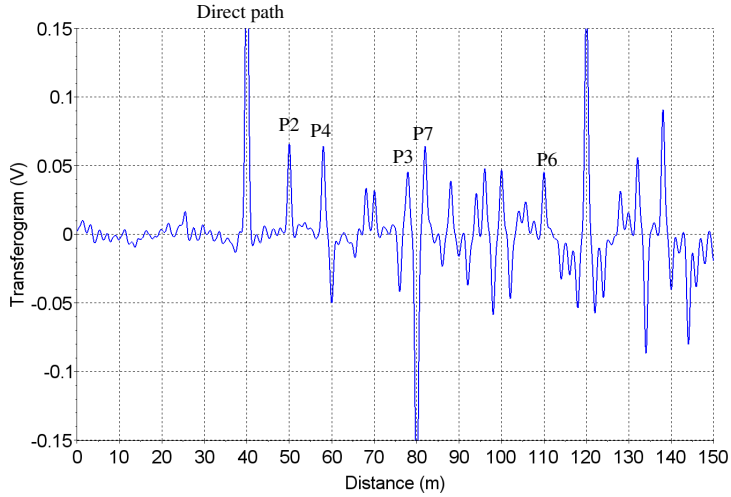

Figure 14. Transferogram from sensor 1 to sensor 5.

In this case, only 2 sensors are necessary to monitor the complete network.

5. DISCUSSION

We discuss here the various cases in which transferometry will prove more efficient than reflectometry.

5.1. Using and Implementing Transferometry

As shown in chapter 2 in Figure 1, using transferometry provides more information than simple or distributed reflectometry. DR requires a communication means between all sensors to aggregate all information and provide a global diagnosis. This is naturally done by transferometry, as the master sensor receives all signals from all the slave sensors. The master only needs to process the incoming signals to provide the global diagnosis result. Of course, a priori knowledge of the network's topology

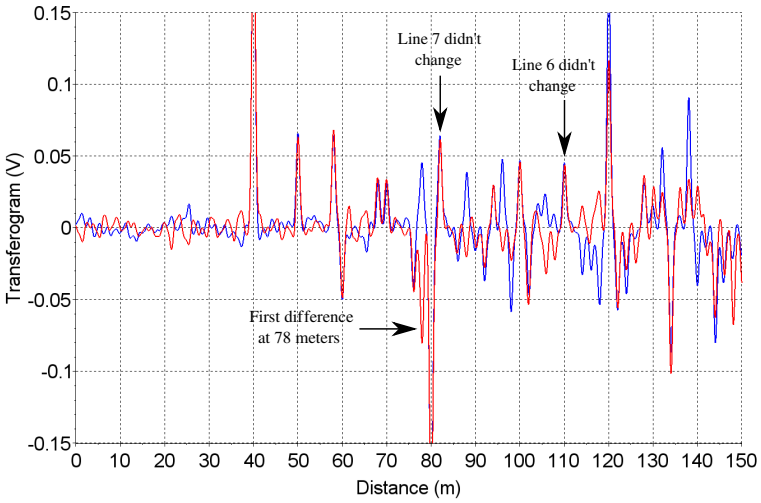

Figure 15. Transferogram from sensor 1 to sensor 5 with a short-circuit at the end of line 3 (blue curve).

is much helpful.

To enable the master to discriminate all the slaves' incoming signals, these signals must have certain properties: if CTDR is chosen [12], orthogonal chaotic signals can easily be generated by each slave sensor using different parameter sets. In this context, orthogonality means that the cross-correlation of the signal is very low, typically less than -30 dB. When the master has finished measuring the incoming signal S, it performs the correlation of this signal with the signal $S_{c,i}$ injected by the slave number i to obtain the associated transferogram τ_i:

$$\tau_i = S \otimes S_{c,i} \quad i = 1 \dots k \tag{20}$$

This implies that the master must have stored all the slaves' signals or is able to generate them. The analysis of the transferograms together with sensor fusion algorithms provide the diagnosis' results [20].

One consequence is that the electronic architecture of the sensors is simplified: slave sensors are simple emitters, and the master's complexity is similar to a standard reflectometer with enhanced processing capacity. If the master additionally does reflectometry, this adds another useful and different information to improve the diagnosis.

Distributed sensors do not need to be synchronized. The master sensor only needs to identify the direct path's peak on each transferogram to set a reference distance: this reference peak is the first and the highest peak on the transferogram. If one knows the network's topology, its amplitude can be computed using simple formulas, to help discriminate it if necessary. Then, as shown in Figures 8 and 9, the difference between the abscissae of this direct path's peak and the defect's peak is twice the distance of the defect to the direct path.

Similar to reflectometry, differential measurements, i.e., comparing the current measure to the reference of the network with no defect or computing the difference between the current measure and the reference, help spot the defect's peak. On the differential curve, the first peak above a chosen threshold is the sought peak. Noticing that some other peaks did not change between the current measure and the reference helps locating the defect's position.

This may imply that the slave sensors inject their signals periodically: a simple rule of thumb is to choose this period equal to 3 times the maximum direct path time among sensors.

Figure 16 displays an example of algorithm for transferometry.

5.2. Advantages of Transferometry

Transferometry is of no use for point-to-point lines diagnosis: it must be used for complex topology networks, where reflectometry will provide complicated or ambiguous results. It will not improve soft

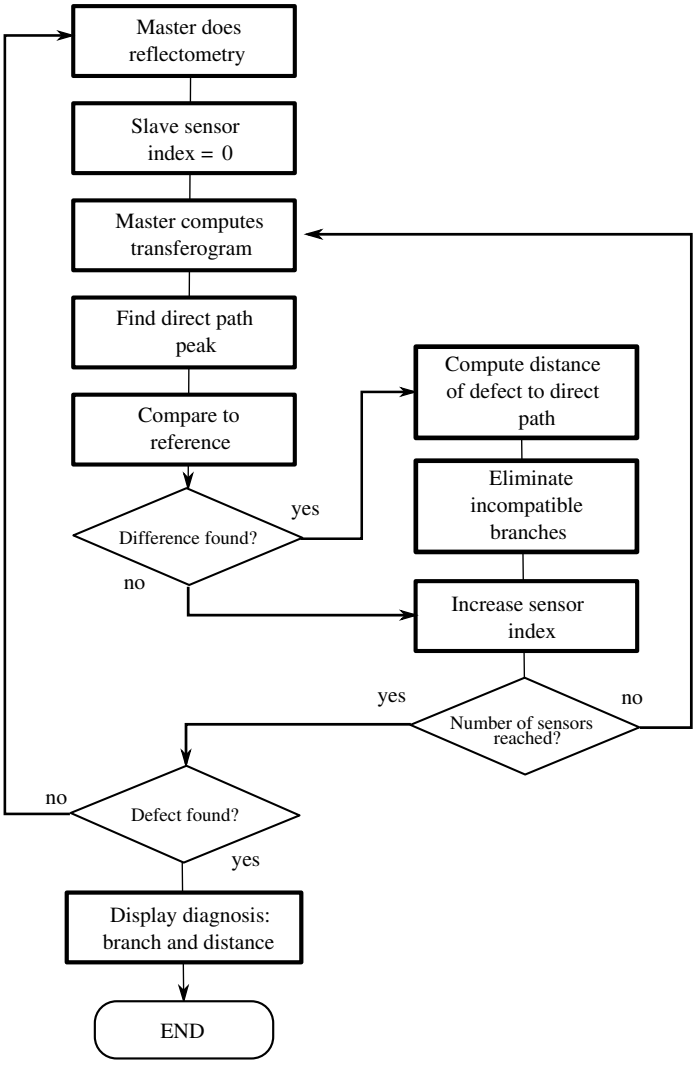

Figure 16. Transferometry algorithm.

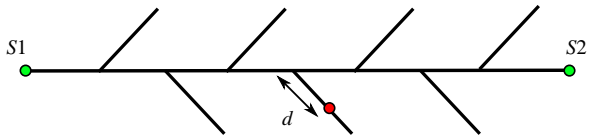

Figure 17. Typical bus network topology.

defects' detection, as the phenomena are the same as in reflectometry.

Section 4 has shown that transferometry is more efficient than reflectometry for bus [20] and star-shaped networks: diagrams are less complex to process. As an example, for the bus topology of Figure 17 equiped with 2 sensors S_1 and S_2 at the green circles, the occurence of a defect on the red dot would create a very low amplitude peak ($T_3^8 = (2/3)^8 \simeq 0.04\,\mathrm{V}$) on the reflectograms in an area containing already a high number of peaks due to multiple paths in all the branches. The defect's peak on the transferogram would be located at the distance $2d$ from the direct path's peak, in a clean zone, with higher amplitude ($T_3^6 \simeq 0.09\,\mathrm{V}$).

Furthermore, transferometry requires less sensors than reflectometry. A bus network with a large number of branches N may only require 2 transferometry sensors while reflectometry needs $N/2$.

6. CONCLUSION

This paper introduces the use of transferometry as an additional tool for the diagnosis of complex topology wired networks. Similar to reflectometry, transferometry takes advantage of the signal produced by electrical waves propagating inside a network to detect and locate possible defects. The main difference is that reflectometry only uses reflected waves when transferometry utilizes transmitted waves, coming from other sensors.

Compared to reflectometry, transferometry's signals are simpler, and the separation power is doubled, because a peak is located at the round-trip distance from the direct path on the transferogram.

In a master-slaves configuration, a single master sensor measures the signal coming from all the slaves, then separates all the signals and processes them to obtain the transferograms. This is made possible using channel access technologies applied to wire diagnosis such as in CTDR. The implementation of transferometry is cheaper compared to distributed reflectometry: the electronic architecture of slave sensors is simplified and the absence of synchronization eases the process. Furthermore, the aggregation of the information from all the computed transferograms ensures a more precise defect detection and location, avoiding position ambiguities. Several case studies have shown that the signal analysis is also simpler than in the case of reflectometry.

On the other hand, one can take advantage of this method to reduce the number of sensors compared to distributed reflectometry, thus reducing the diagnosis' cost. Transferometry has been shown as suited for monitoring bus- and star-shaped networks, topologies that are usually too complex for reflectometry. Monitoring bus network using reflectometry requires at least that half the line ends have a sensor, but this number can be drastically reduced using transferometry, where only 2 sensors (one at each extremity) may be enough. For more complex topologies, the decomposition in bus and star sub-networks provides an initial guess for sensors positionning. This can further be refined using numerical simulations with specifically or randomly placed defects.

This method requires deeper studies and experimentations to emphasize its advantages. Testing its application to the diagnosis of intermittent defects would also be interesting.

REFERENCES

1. Auzanneau, F., "Wire troubleshooting and diagnosis: Review and perspectives," *Progress In Electromagnetics Research B*, Vol. 49, 253–279, 2013.
2. Li, H., A. Bose, and V. M. Venkatasubramanian, "Wide-area voltage monitoring and optimization," *IEEE Transactions on Smart Grid*, Vol. 7, No. 2, 785–793, 2016.
3. Tudor, J., D. Stevens, G. Ott, and W. Pomeroy, "Frequency modulated fault locator for power lines," *IEEE Transactions on Power Apparatus and Systems*, Vol. 95, 1760–1768, 1972.
4. Lelong, A., M. Olivas Carrion, V. Degardin, and M. Lienard, "On line wire diagnosis by modified spread spectrum time domain reflectometry," *PIERS Proceeding*, 182–186, Cambridge, USA, July 2–6, 2008.
5. Lelong, A. and M. Olivas Carrion, "On line wire diagnosis using multcarrier time domain reflectometry for fault location," *IEEE Sensors Conference*, 751–754, Christchurch, New Zealand, August 2009.
6. Ben Hassen, W., F. Auzanneau, F. Peres, and A. Tchangani, "OMTDR using BER estimation for ambiguities cancellation in ramified networks diagnosis," *IEEE ISSNIP Conference*, Melbourne, Australia, April 2013.
7. Furse, C., R. Dangol, and R. Nielsen, "Frequency-domain reflectometry for on-board testing of aging aircraft wiring," *IEEE Transactions on Electromagnetic Compatibility*, Vol. 45, No. 2, 306–315, 2003.
8. Sallem, S., and N. Ravot, "Self-adaptive correlation method for soft defect detection in cable by reflectometry," *Proceeding of 2014 IEEE Sensors Conference*, 2114–2117, Valencia, Spain, November 2014.

9. Sommervogel, L., L. El Sahmarany, and L. Incarbone, "Method to compensate dispersion effect applied to time domain reflectometry," *Electronics Letters*, Vol. 49, No. 18, 1154–1155, August 2013.
10. Ravot, N., F. Auzanneau, Y. Bonhomme, M. Olivas Carrion, and F. Bouillault, "Distributed reflectometry-based diagnosis for complex wired networks," *EMC: Safety, Reliability and Security of Communication and Transportation Systems, EMC Workshop*, Paris, June 2007.
11. Ben Hassen, W., F. Auzanneau, F. Peres, and A. Tchangani, "A distributed diagnosis strategy using bayesian network for complex wiring networks," *IFAC A-MEST Workshop*, Sevilla, Spain, November 2012.
12. Auzanneau, F., "Chaos time-domain reflectometry for distributed diagnosis of complex topology wired networks," *Electronics Letters*, Vol. 52, No. 4, 280–281, February 2016.
13. Fink, M., "Time reversal of ultrasonic fields — Part 1: Basic principles," *IEEE Trans. Ultrasonics, Ferroelectrics, and Frequency Control*, Vol. 39, No. 5, 555–566, September 1992.
14. Abboud L., A. Cozza, and L. Pichon, "A noniterative method for locating soft faults in complex wire networks," *IEEE Transactions on Vehicular Technology*, Vol. 62, No. 3, 1010–1019, March 2013.
15. Kafal M., A. Cozza, and L. Pichon, "Locating multiple soft faults in wire networks using an alternative DORT implementation," *IEEE Transactions on Instrumentation and Measurement*, Vol. 65, No, 2, 399–406, Februry 2016.
16. Miao G., J. Zander, K.-W. Sung, and B. Slimane, *Fundamentals of Mobile Data Networks*, Cambridge University Press, 2016.
17. Auzanneau, F., M. Olivas Carrion, and N. Ravot, "A simple and accurate model for wire diagnosis using reflectometry," *PIERS Proceedings*, 232–236, Prague, Czech Republic, August 27–30, 2007.
18. Beck G., S. Imperiale, and P. Joly, "Mathematical modelling of multi conductor cables," *Discrete and Continuous Dynamical Systems — Series S (DCDS-S)*, Vol. 8, No. 3, 521–546, 2015.
19. Ulrich, M. and B. Yang, "Inference of wired network topology using multipoint reflectometry," *Proc. of 23rd European Signal Processing Conf. EUSIPCO*, Nice, France, August 2015.
20. Ben Hassen, W., F. Peres, and A. Tchangani, "Diagnosis sensor fusion for wire fault location in CAN bus systems," *IEEE Sensors Conference*, Baltimore, USA, November 2013.
21. Visco Comandini, F., M. Sorine, and M. Mirrahimi, "On the inverse scattering of star-shape LC-networks" *Proceedings of the IEEE Conference on Decision and Control*, 2075–2080, Cancun, Mexico, December 2008.